Sub-symbol Based Carrier Phase Recovery in CO-OFDM System with Linear Interpolation

Xiaojian Hong, Xuezhi Hong, and Sailing He
ZJU-SCNU Joint Research Center of Photonics
South China Normal University (SCNU), Guangzhou 510006, China

Abstract— A novel optical carrier phase recovery algorithm using phase linear interpolation and sub-symbol processing is proposed for CO-OFDM system. Compared with the conventional carrier phase recovery approach, the new algorithm can promote the system's laser linewidth tolerance significantly with increased temporal resolution in tracking the carrier phase.

1. INTRODUCTION

Coherent optical orthogonal frequency division multiplexing (CO-OFDM) has been intensively studied for its high tolerance to chromatic dispersion (CD) and polarization mode dispersion (PMD) [1–3]. However, the performance degradation caused by laser phase noise is more pronounced in CO-OFDM system compared with the single carrier counterpart. In CO-OFDM system, laser phase noise degrades the received signal quality in two ways: the common phase error (CPE) and the inter-carrier-interference (ICI). The former one causes an identical phase rotation for all subcarriers while the latter one induces frequency dependent noise for each subcarrier channel. To suppress these distortions, pilot subcarrier aided (PA) carrier phase recovery technique is widely applied because of its simplicity [2–5]. In PA CPE compensation (CPEC) scheme [2, 3], symbol rotation is corrected while the ICI is left uncompensated as laser phase noise is assumed to be constant in one CO-OFDM symbol. However, for relatively large laser linewidth and/or long symbol duration scenarios, the degradation due to ICI becomes pronounced and need to be compensated. In [4, 5], partial ICI suppression is achieved by temporal linear interpolation (LI) of CPE in the adjacent symbols. In [6], frequency domain orthogonal basis expansion-based method (OBE) has been proposed to suppress both CPE and partial ICI, in which complex matrix inversion operation is needed.

To improve the ICI tolerance of CO-OFDM system, we proposed a carrier phase recovery method based on sub-symbol processing in our former paper [7], in which a full CO-OFDM symbol is temporally partitioned into several blocks (i.e., sub-symbols) to obtain a high temporal resolution of carrier phase recovery. In this paper, we propose a novel carrier phase recovery algorithm based on linear interpolation and sub-symbol processing. By combining the above two ingredients, a better tracking of the carrier phase can be achieved with the new algorithm compared to the former one [7]. The principle and feasibility of our proposal are shown in the following sections. Performance evaluation and key parameter optimization are conducted with Monte-Carlo simulation.

2. PROPOSED CARRIER PHASE RECOVERY SCHEME

2.1. PSystem Model and Notation

The schematic diagram of our proposed algorithm is depicted in Fig. 1. The nth element of the mth vector is denoted by x_n^m/X_n^m in time/frequency domain, respectively. The signal model in the presence of phase noise is studied in [2]. At the nth signal sample of the mth OFDM symbol, laser phase noise introduces a random phase rotation of $e^{j\phi_n^m}$ in the time domain where $\phi_n^m = \phi_{n-1}^m + u$ and $u \sim N\ (0, \sigma_u^2)$. The phase noise variance is $\sigma_u^2 = 2\pi\beta T_s$ where T_s is the CO-OFDM symbol duration, β is the two-side 3-dB bandwidth of the laser phase noise.

After coherent detection, the phase noise of the free-running lasers at the transmitter and the receiver is linearly transferred from optical domain to electrical domain. The O/E converted signal is sampled and digitalized by the analog-to-digital converter (ADC). Several digital signal processing (DSP) functions are then executed to recover the transmitted data. Firstly, the cyclic prefix (CP) of signal is removed and frequency offset is compensated digitally. The signal is then converted to frequency domain by fast Fourier transform (FFT). The effect of phase noise on CO-OFDM system after frequency offset compensation can be expressed as a convolution in the frequency domain.

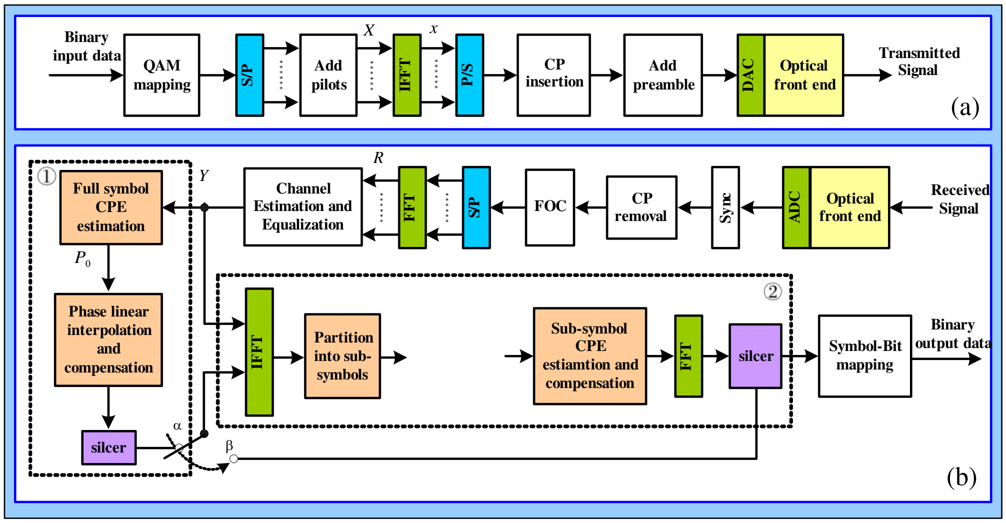

Figure 1: Schematic diagram of CO-OFDM, (a) transmitter and (b) receiver with proposed phase noise suppression algorithm. S/P: serial-to-parallel conversion; P/S: parallel-to-serial conversion; Sync: synchronization. FOC: frequency offset compensation.

Assuming that both timing synchronization and frequency tracking are perfectly performed, the received signal R can be expressed as [5]:

$$R_k^m = \sum_{q=0}^{N-1} P_{\langle k-q\rangle}^m H_q X_q^m + W_k^m = P_0^m H_k X_k^m + \sum_{q=0,q\neq k}^{N-1} P_{\langle k-q\rangle}^m H_q X_q^m + W_k^m\text{: } 0 \leq k \leq N-1 \tag{1}$$

where N is the number of subcarriers, X, P, H and R are the transmitted data symbol, the phase noise spectral components, the channel frequency response and the received data symbol in frequency-domain, respectively. The notation $\langle\cdot\rangle$ denotes the modulo-N operation and W is the additive Gaussian distributed noise with zero mean and variance σ_u^2. The kth phase noise spectral component of the mth symbol P_k^m, can be written as:

$$P_k^m = \frac{1}{N}\sum_{n=0}^{N-1} e^{j\phi_n^m} \exp\left(-\frac{j2\pi nk}{N}\right) : 0 \leq k \leq N-1. \tag{2}$$

As seen in (1), the first part P_0^m is the common term influencing all subcarriers, therefore, representing the CPE contribution. The second part $\sum\limits_{q=0,q\neq k}^{N-1} P_{\langle k-q\rangle}^m H_q X_q^m$ stands for the contribution of ICI.

2.2. Carrier Phase Recovery Algorithm

After channel estimation and equalization, two types of processes are performed: one is the 'full symbol linearly interpolated carrier phase estimation process' and the other one is the 'sub-symbol phase noise suppression process'. The second process can be executed iteratively until a predetermined number of iteration is completed to obtain a better phase noise suppression effect.

In the first process, the pilot subcarriers are used to estimate the CPE in every full OFDM data symbol. The least-squares (LS) algorithm can be used to estimate CPE as follow:

$$CPE^m = angle(P_0^m) = angle\left\{\frac{\sum_{k\in S_p}(X_k^m)^* Y_k^m}{\sum_{k\in S_p}\left|X_k^m\right|^2}\right\} \tag{3}$$

where S_p is the set of the subcarriers indices corresponding to the pilot subcarriers.

The carrier phase at the middle of the corresponding symbol is set equal to the estimated CPE. The carrier phase of the remaining intermediate temporal sample is obtained by linear interpolating the CPE estimation of the adjacent symbols. As can be seen from Fig. 2, the equalization of the

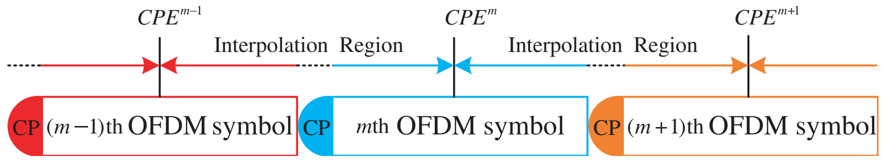

Figure 2: Diagram of phase linear interpolation with three adjacent CO-OFDM symbols.

mth received symbol can be completed only after reception of the $(m+1)$th symbol which results in one symbol latency.

The carrier phase is compensated coarsely using the interpolated estimation. After tentative decision on coarsely compensated samples, the second stage carrier phase recovery is processed. In the second stage, the output from the slicer $\hat{X}$ and channel equalized samples Y are converted back to time domain by using IFFT operation and then partitioned into several sub-symbols. After taking the normalized S-point FFT operation on the sub-symbol samples, sub-symbol CPE estimation is processed by comparing the phase of the "recovered" temporal samples $\hat{X}_k^b$ and the channel equalized temporal samples $\hat{Y}_k^b$ using LS algorithm.

$$\hat{P}_0^b = \frac{\sum_{k=0}^{S-1} (\hat{X}_k^b)^* \hat{Y}_k^b}{\sum_{k=0}^{S-1} \left|\hat{X}_k^b\right|^2} \tag{4}$$

where S is the length of the sub-symbol. The estimated sub-symbol CPE values are then used to update the carrier phase of every sample. Finally, the phase corrected data is decision and mapped from symbol to bits.

3. SIMULATION RESULTS AND DISCUSSIONS

The proposed algorithm is assessed through Monte-Carlo simulation. We use 'LI-SCPEC' to refer to the proposed algorithm. The parameters of simulated CO-OFDM system are as follows. The mapped 16-QAM signal is converted to time domain by 256-point IFFT. 40 guard sub-carriers are added and allocated at both side of the band. 10 pilots are uniformly inserted into each block. The CP length is 32. The sampling rate R_s is 10 GSamples/s. Thus the duration of OFDM symbol is 28.8 ns. Ideal frequency offset compensation and channel equalization are assumed in the simulation to obtain an accurate laser phase noise tolerance measurement.

The bit error rate (BER) versus optical signal to noise ratio (OSNR) curves using different algorithms for 250 kHz laser linewidth are show in Fig. 3(a). At 20 dB OSNR, the BER of LI-SCPEC ($N_B = 1$), LI-SCPEC ($N_B = 2$) and LI-SCPEC ($N_B = 4$) are 4.17e-4, 6.4e-5 and 4.85e-5, respectively, which show that the performance improvement increases as N_B from 1 to 2, 4. When comparing with the full symbol decision-feedback algorithm (DF-CPEC) which have a comparable complexity, the corresponding sub-symbol algorithm offer 2.06 dB ($N_B = 2$) and 2.36 dB ($N_B = 4$) OSNR gain at BER = 1.0e-3.

In Fig. 3(b), we compare the required OSNR at BER = 1.0e-3 as a function of combined laser linewidth. For comparison, the performance of CPEC algorithm in [2], LI algorithm in [5] and previous sub-symbol algorithm SCPEC in [7] are also show in Fig. 3(b). The laser linewidth tolerance is evidently improved by the LI-SCPEC algorithm. For laser linewidth of 250 kHz, the required OSNR of CPEC, LI, DF-CPEC, SCPEC ($N_B = 2$) are 24.1 dB, 20.38 dB, 18.69 dB and 17.57 dB, while 16.63 dB for LI-SCPEC ($N_B = 2$). The advantage of LI-SCPEC method tends to be larger when the laser linewidth increases. For OSNR = 20 dB, the system's laser linewidth tolerance is about 154 kHz (CPEC), 230 kHz (LI), 298 kHz (DF-CPEC), 382 kHz (SCPEC, $N_B = 2$) and 541 kHz (LI-SCPEC, $N_B = 2$). Thus, LI-SCPEC algorithm promotes system tolerance of laser phase noise evidently.

The contour plot of the receiver sensitivity (in OSNR) penalty at BER = 1.0e-3 are depicted in Fig. 4(a) for LI-SCPEC with respect to different laser linewidth ($0 \sim 345$ kHz) and different number of sub-symbols N_B ($1 \leq N_B \leq 6$). The reference is the OSNR at BER = 1.0e-3 in ideal coherent detection with perfect carrier phase recovery. For a certain range ($0 \sim 200$ kHz), there exist an optimal number of sub-symbol. The OSNR penalty drops with increasing number of sub-symbols (≤ 6) if the linewidth > 250 kHz. A few number of sub-symbols (≤ 4) is sufficient to obtain a

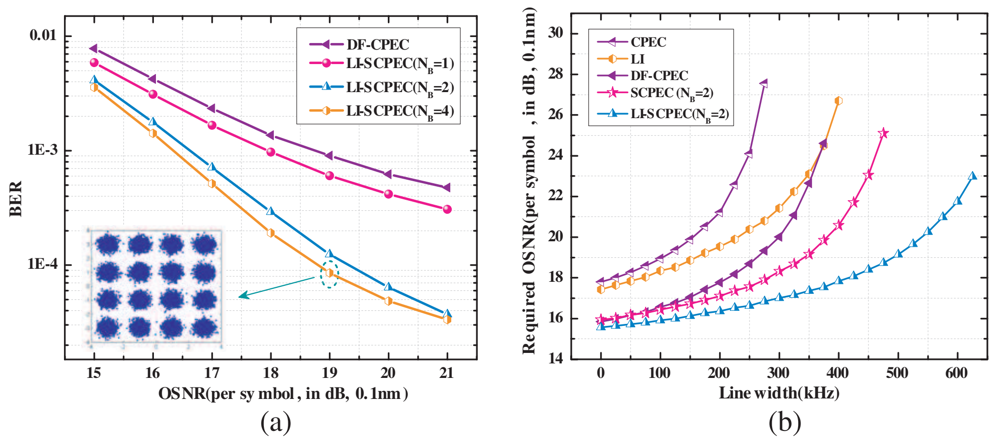

Figure 3: (a) BER performance in B2B case for laser linewidth = 250 kHz, inset shows the corresponding constellation, (b) required OSNR at BER =1.0e-3 with different carrier phase recovery algorithms.

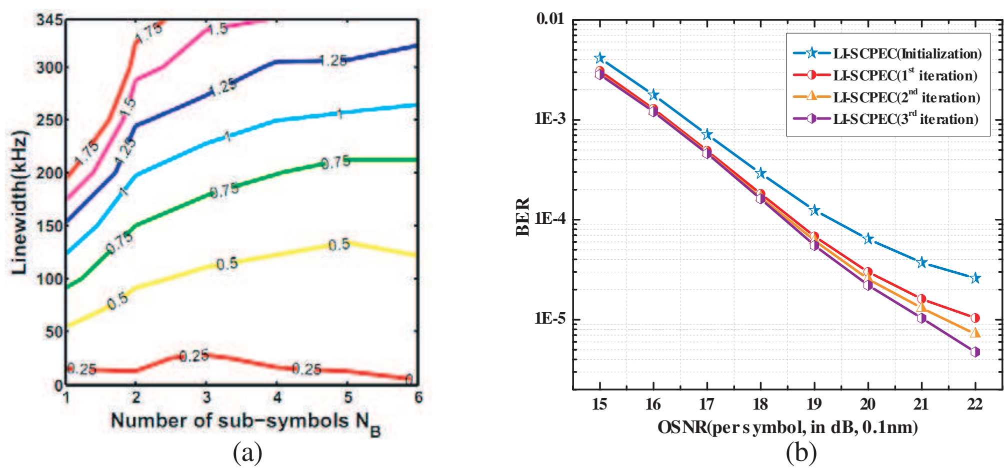

Figure 4: (a) Receiver sensitivity penalty at 1.0e-3 versus the different laser linewidth and different number of sub-symbols NB, (b) BER versus OSNR curves for the proposed carrier phase recovery algorithm after iteration.

moderate OSNR penalty ($\leq$ 1.5 dB) for a large interval of laser linewidth (0 $\sim$ 345 kHz), which relieves the complexity requirement of our algorithm.

The BER performance of proposed algorithm after iteration is shown in Fig. 4(b). The performance of CO-OFDM system (linewidth = 250 kHz, N_B = 2) is improved by iteration. The iteration gain at BER = 1.0e-3 is 0.365 dB, 0.418 dB, 0.431 dB for number of iteration = 1, 2 and 3, respectively. Note that the curves almost converge after the first time of iteration, which implies that the number of iteration = 1 is enough to obtain a reasonable improvement.

4. CONCLUSION

In this paper, we propose a novel carrier phase recovery method based on linear interpolation and sub-symbol processing. The accuracy of sub-symbol carrier phase estimation is improved by linear interpolation. The effectiveness of proposed method is evaluated by simulation which shows that the system's laser linewidth tolerance can be enhanced significantly. The optimized performance of the algorithm can be achieved with a moderate number of sub-symbols and a small number of iteration.

ACKNOWLEDGMENT

This work is supported by the China Postdoctoral Science Foundation (No. 2013M531868), Guangdong Innovative Research Team Program (No. 201001D0104799318) and Young Faculty Research Fund of SCNU (No. 13KJ04).

REFERENCES

1. Shieh, W. and I. Djordjevic, *OFDM for Optical Communications*, ELSEVIER, USA, 2009.
2. Yi, X., W. Shieh and Y. Ma, "Phase noise effect on high spectral efficiency coherent optical OFDM transmission," *IEEE Journal of Lightwave Technology*, Vol. 26, No. 10, 1309–1316, 2008.
3. Yi, X., W. Shieh, and Y. Tang, "Phase estimation for coherent optical OFDM," *IEEE Photonics Technology Letters*, Vol. 19, No. 12, 919–921, 2007.
4. Rabiei, P., W. Namgoong and N. Al-Dhahir, "A non-iterative technique for phase noise ICI mitigation in packet-based OFDM systmes," *IEEE Transactions on Signal Processing*, Vol. 58, No. 11, 5945–5950, 2010.
5. Mousa-Pasandi, M. E. and D. V. Plant, "Non-iterative interpolation-based partial phase noise ICI mitigation for CO-OFDM transport systems," *IEEE Photonics Technology Letters*, Vol. 23, No. 21, 1594–1596, 2011.
6. Fang, X., C. Yang, T. Zhang, and F. Zhang, "Orthogonal basis expansion-based phase noise suppression for PDM CO-OFDM system," *IEEE Photonics Technology Letters*, Vol. 26, No. 4, 376–379, 2014.
7. Hong, X. and S. He, "Sub-frame carrier phase estimation for coherent optical orthogonal frequency multiplexing system," *Progress In Electromagnetics Research Symposium Abstracts*, 314–315, Stockholm, Sweden, August 314-315, 2013.